

1 **Prognosticating Mesothelioma Using Predictive Analytics**

2
3 **Avishek Choudhury**
4 Research Assistant
5 School of Systems and Enterprises
6 Stevens Institute of Technology
7 <https://orcid.org/0000-0002-5342-0709>
8 ResearcherID: P-2415-2018

9 **Correspondence:**

10 Avishek Choudhury (Research Assistant)

11 School of Systems and Enterprises

12 Stevens Institute of Technology

13 Hoboken, USA

14 Email: achoudh7@stevens.edu

15 Mobile: +1 (515) 608-0777

16

17

18

19

20

21

22

23



24 Prognosticating Mesothelioma Using Predictive Analytics

25 Abstract

26 **Background:** Malignant pleural mesothelioma (MPM) is an atypical, belligerent tumor that
27 matures into cancer in the pleura, a stratum of tissue bordering the lungs. Pleural mesothelioma is
28 a common type of mesothelioma that accounts for about 75 percent of all mesothelioma diagnosed
29 yearly in the United States. Diagnosis of mesothelioma takes several months and is expensive.
30 Given the difficulty of diagnosing MPM, early identification is crucial for patient survival. Our
31 study implements artificial intelligence and recommends the best fit model for early diagnosis and
32 prognosis of MPM. **Method:** We retrospectively retrieved patient's medical reports generated by
33 Dicle University, Turkey and implemented multi-layered perceptron (MLP), voted perceptron
34 (VP), Clojure classifier (CC), kernel logistic regression (KLR), stochastic gradient decent SGD),
35 adaptive boosting (AdaBoost), Hoeffding tree (VFDT), and primal estimated sub-gradient solver
36 for support vector machine (s-Pegasos). We evaluated the models, compared and tested using
37 *paired T – test (corrected)* at 0.05 significance based on their respective classification
38 accuracy, f-measure, precision, recall, root mean squared error, receivers characteristic curve
39 (ROC), and precision-recall curve (PRC). **Results:** In phase-1 SGD, AdaBoost.M1, KLR, MLP,
40 VFDT generates optimal results with the highest possible performance measures. In phase-2,
41 AdaBoost with a classification accuracy of 71.29% outperformed all other algorithms. C-reactive
42 protein, platelet count, duration of symptoms, gender, and pleural protein were found to be the
43 most relevant predictors that can prognosticate mesothelioma. **Conclusion:** This study confirms
44 that data obtained from biopsy and imagining tests are strong predictors of mesothelioma but are
45 associated with high cost, however, can identify mesothelioma with optimal accuracy. Predictive
46 analytics without using biopsy results can diagnose mesothelioma with acceptable accuracy.

47 Implementation of phase-2 followed by phase-1 can address diagnosis expenses and maximize
48 disease prognosis. Additionally, results indicate improved MPM diagnosis using AI methods
49 dependent upon the specific application.

50

51 **Keywords:** Mesothelioma; Predictive modeling; Decision support system; Early diagnosis.

52

53

54

55

56

57

58

59

60

61

62

63

64

65

66

67

68

69

70

Prognosticating Mesothelioma Using Predictive Analytics

1. Background

72 Malignant pleural mesothelioma (MPM) is a hostile tumor of mesothelial cells concomitant with
73 preceding asbestos contact. With an amplified implementation of chemotherapy (Vogelzang,
74 Rusthoven, Symanowski, & al., 2003) (Zalcman, et al., 2016) and a varied gamut of clinical
75 examinations, precise prognostication is a crucial subject for individuals with MPM, doctors, and
76 scholars. However, MPM is an outstandingly different ailment. Staging system (Pass, Giroux,
77 Kennedy, & al., 2016), challenging primary tumor identification process (Gill, Naidich, Mitchell,
78 & al., 2016;) (Frauenfelder, Tutic, Weder, & al., 2011;) and distinct biology (Bueno, Stawiski,
79 Goldstein, & al., 2016;), impedes accurate prediction. MM is a rare disease; it affects about two
80 individuals per million per annum in a general population (McDonald, C., & McDonald., 1996).
81 Comparatively industrialized nations are affected more by MM (Spirtas, et al., 1986;) (Peto,
82 Hodgson, Matthews, & Jones, 1995;) (Leigh, et al., 1991;) due to higher exposure to asbestos
83 (Metintas, et al., 2008). Severity of mesothelioma can be categorized into stage 1, stage 2, stage 3,
84 and stage 4 (cancer). Stage1 and stage 2 symptoms of MPM such as dry coughing, dyspnea,
85 respiratory complications, chest or abdominal pain, fever, pleural effusion, fatigues, and muscle
86 weakness are very weak predictors of mesothelioma (Mesothelioma News, 2018). Since
87 mesothelioma is rare, patients are less likely to be suspected with the disease. Moreover, its initial
88 symptoms during stage 1 and 2 resemble other diseases such as pneumonia or irritable bowel
89 syndrome (Selby, 2018), MM can also be mistaken for an infection or a more common type of
90 non-terminal lung cancer that develops in mucus-secreting glands called adenocarcinoma (Selby,
91 2018). If mesothelioma is not diagnosed and meets no medical aid at its premature stage, it rapidly
92 burgeons into a stage 3 or stage 4 cancer. Unfortunately, the survival rate after being diagnosed

93 with late stage mesothelioma is typically about a year. In order to treat mesothelioma effectively,
94 an early diagnosis is recommended.

95 Diagnosing mesothelioma is challenging, and the expenses associated with identifying this disease
96 can ascend rapidly. In fact, since the principal way to diagnose mesothelioma incorporates ruling
97 out other plausible diseases, more frequently than not, many examinations may be administered
98 that aren't exclusive to mesothelioma itself but are for erstwhile disorders instead (Molinari, 2018).
99 Furthermore, it is often suggested to get a second opinion (Molinari, 2018), recapping many of the
100 diagnostic tests over and over. For all these causes, diagnostic expenses for mesothelioma starts
101 piling up even before the required treatment commences. Mesothelioma diagnosis typically
102 implicates taking imaging scans of tumors, examining a biopsy of cancer tissue, and blood tests
103 (Selby, 2018).

104 Oncologists use imaging tests to look for noticeable signs of tumors. A mesothelioma diagnosis
105 depends on a series of diagnostic imaging tests, including X-rays, CT scans, MRIs and PET scan
106 (Selby, 2018) all of which are expensive.

107 Two chief factors make imaging tests expensive. Foremost, the specialized imaging equipment is
108 expensive both for an upfront purchase and for maintenance. Secondly, this equipment requires
109 well-trained technicians to ensure apt operation of the device. A patient can presume to spend
110 about \$800 – \$1,600 (Molinari, 2018) for a single CT, MRI, or PET scan respectively. Moreover,
111 multiple scans may be required during diagnosis (Molinari, 2018), which can quickly burgeon
112 the overall costs.

113 The most accurate test for confirming mesothelioma is a biopsy (Selby, 2018). It is a procedure
114 that requires removal of fluid or tissue samples from the tumor or cancer site and their analysis
115 under a microscope. There are many diverse approaches to obtaining a biopsy, and which one to

116 be used depends on the suspected tumors' location. Some biopsies embrace making an incision and
117 inserting implements to obtain a sample of the tumor cell, while others only require a needle. Given
118 the wide range of biopsy procedures, its expenses can range from \$500 to \$700 for a needle biopsy
119 (Molinari, 2018), \$3,600 to \$ 5000 for pleuroscopy (lungs) or laparoscopy (abdomen) (Molinari,
120 2018), \$7,800 to \$7,900 for thoracotomy (lungs) or laparotomy (abdomen) (Molinari, 2018). Like
121 other diagnostic procedures, biopsies may also require to be performed multiple times (Molinari,
122 2018), increasing the overall diagnosis expenses. Doctors also explore a variety of blood tests such
123 as MESOMARK, SOMAmer, and Human MPF to look for biomarkers that suggest mesothelioma
124 (Selby, 2018). However, currently, no blood tests are precise enough to confirm a diagnosis on
125 their own (Selby, 2018).

126 **2. Problem statement**

127 Malignant Pleural mesothelioma has the potential to grow into cancer and sabotage patient health.
128 Like any other fatal disease, malignant mesothelioma demands early diagnosis and effective
129 treatment. However, effective diagnosis methods such as thoracotomy and pleuroscopy are costly
130 and might not be affordable for patients worldwide (Friedin, 2012) (Pope, 2010). Additionally,
131 about two third of the world do not have adequate access to the required technologies, expensive
132 imaging devices, and expert technicians (Silvester, 2016).

133 There exists some work of literature that has used artificial intelligence or machine learning
134 algorithms such as decision tree, random forest, support vector machine, and even artificial neural
135 network to identify MM (Choudhury , Identification of Cancer: Mesothelioma's Disease Using
136 Logistic Regression and Association Rule, 2018) (Ilhan & Celik, 2016) but with some limitations.
137 These models (random forest, decision tree, and others) either tend to overfit (Tin, 1995) or fails
138 to generate 100% accuracy or might also fail to converge a large dataset (Lotfi & Keshavarz, 2014).

139 In our study, we propose a model that overcome the aforementioned flaws and can diagnose MM
140 with and without requiring data from expensive biopsy and imaging tests.

141 **3. Methodology**

142 Our study uses the patient's medical reports generated by Dicle University. The dataset contains
143 34 attributes, one binary response variable, and 324 instances. It consists of 41% females and 59%
144 males. The patients involved in this study were in nine different cities. We performed k-fold cross-
145 validation to minimize any bias and variance in the dataset. Cross-validation is a resampling
146 technique used to gauge machine learning models on a limited dataset. In this method, the original
147 data sample is randomly partitioned into k proportional subsamples. Of the k subsamples, one
148 subsample is retained as the validation data for evaluating the model, and the remaining $k-1$
149 subsamples are used as training data. The cross-validation process is then reiterated k times. The k
150 results obtained from the k -folds are then averaged to produce a single estimation. In this study we
151 considered the value of k to be 10 becoming 10-fold cross-validation. The selection of k is usually
152 5 or 10 (Kuhn & Johnson, 2018). There is a bias-variance trade-off related to the value of k in k -
153 fold cross-validation. Performing k -fold cross-validation using $k = 5$ or $k = 10$ have empirically
154 shown to yield test error rate estimates that free from extreme high bias and variance (James,
155 Witten, Hastie, & Tibshirani, 2017). All the analysis was performed using R-studio, an open source
156 machine learning and statistical tool, and *Waikato Environment for Knowledge Analysis* (WEKA),
157 a free software suite of machine learning licensed under the GNU General Public License,
158 programmed in JAVA, and developed at the University of Waikato, New Zealand.

159 Table 1 below lists all the attributes contained in our dataset, it also determines the mean, deviation
160 and logistic correlation of all predictors with the target variable ("class of diagnosis"). In
161 classification applications, calculating logistic dependencies between a single input and single

162 target or class variable is essential. It determines the absolute values of the logistic correlation
 163 between all inputs and all targets. The logistic correlation is a numerical value between *zero* and
 164 *one* that expresses the strength of the logistic relationship between a single input and output
 165 variables. A value close to *one* indicates a healthy relationship and value approaching *zero* denotes
 166 weak or no relationship.

167

Table 1: Data Statistics

| Predictor | Mean | Deviation | Logistic correlation with the target variable ("class of diagnosis") |
|-------------------------------|---------|-----------|--|
| Age | 54.74 | 11.00 | 0.06 |
| Gender | - | - | 0.15 |
| City | NA | NA | 0.02 |
| Asbestos exposure | 0.86 | 0.34 | 0.07 |
| Type of MM | 0.05 | 0.26 | 0.13 |
| Duration of asbestos exposure | 30.18 | 16.41 | 0.06 |
| Diagnosis method* | - | - | 1.00* |
| Keep side | 0.75 | 0.56 | 0.10 |
| Cytology | 0.28 | 0.45 | 0.02 |
| Duration of symptoms | 5.44 | 4.71 | 0.02 |
| Dyspnea | 0.81 | 0.38 | 0.02 |
| Ache on chest | 0.68 | 0.46 | 0.05 |
| Weakness | 0.61 | 0.48 | 0.06 |
| Habit of cigarette | 0.91 | 1.15 | 0.05 |
| Performance status | 0.52 | 0.50 | 0.03 |
| White blood | 9457.45 | 3450.73 | 0.05 |
| Cell count (WBC) | 9.55 | 3.34 | 0.05 |
| Hemoglobin (HGB) | 0.42 | 0.49 | 0.03 |
| Platelet count (PLT) | 369.65 | 227.55 | 0.06 |
| Sedimentation | 70.68 | 21.74 | 0.00 |

| | | | |
|----------------------------------|--------|--------|------|
| Blood lactic dehydrogenize (LDH) | 308.91 | 185.14 | 0.01 |
| Alkaline phosphate (ALP) | 66.16 | 35.07 | 0.04 |
| Total protein | 6.58 | 0.82 | 0.01 |
| Albumin | 3.30 | 0.63 | 0.04 |
| Glucose | 112.41 | 38.46 | 0.01 |
| Pleural lactic dehydrogenize | 518.47 | 536.27 | 0.03 |
| Pleural protein | 3.93 | 1.57 | 0.03 |
| Pleural albumin | 2.07 | 0.91 | 0.07 |
| Pleural glucose | 48.44 | 27.23 | 0.01 |
| Dead or not | - | - | - |
| Pleural effusion | 0.87 | 0.33 | 0.03 |
| Pleural thickness on tomography | 0.59 | 0.49 | 0.01 |
| Pleural level of acidity (pH) | 0.52 | 0.50 | 0.04 |
| C reactive protein (CRP) | 64.18 | 22.66 | 0.11 |

***Diagnosis method contains data obtained from biopsy and imaging tests. It contains binary values where 1= biopsy or imaging test indicates MM; 0 = otherwise.**

168 Mesothelioma data set can be broadly divided into pre-diagnosis data and post-diagnosis
169 data. Pre-diagnosis data refers to the all the records obtained before mesothelioma was clinically
170 confirmed such as patient age, gender, the city they belonged to, smoking habit, exposure to
171 asbestos, duration of exposure to asbestos, early-stage symptoms including the feeling of
172 weakness, heartache, and dyspnea, and duration of symptoms. Pre-diagnosis data also
173 encompasses blood test results such as white blood cell count, hemoglobin level, platelets count
174 and others.

175 Post-diagnosis are those data that refers to the records retrieved after mesothelioma was
176 confirmed. Type of mesothelioma detected (type of MM), side effects of chemotherapy (keep

177 side), and survival of the patient after treatment (dead or not) are all post-diagnosis data. This study
178 eliminates the "dead or not" predictor from all analysis.

179 Table 1 above indicates that the predictor "diagnosis method" is strongly correlated with
180 the target variable. The predictor "diagnosis method" refers to data obtained from invasive biopsy,
181 and imaging test results. Invasive biopsy and imaging tests can accurately identify mesothelioma
182 but are expensive procedures and may require repeated examinations as stated earlier. To advocate
183 the applicability of AI predictive analytics on both pre and post diagnostic data we perform a
184 comparative analysis of classification models into two phases. Phase-1 models use all the predictor
185 variables except "dead or not" as input to produce high classification accuracy. The same set of
186 models in Phase-2 only takes relevant predictors from pre-diagnosis data as its input.

187 Phase-1 and phase-2 are denoted as *high accuracy* and *low-cost* phases respectively
188 because phase-1 execution demands data from expensive, invasive biopsy and imaging test results
189 which are robust predictors of MM (logistic correlation = 1) and thus the model is expected to
190 yield high accuracy. Whereas, phase-2 considers only predictors with lower logistic correlation
191 (pre-diagnosis data) and eliminates the use of invasive biopsy and imaging test results. Execution
192 of phase-2 also incorporates a feature selection method to enhance its accuracy and reduce
193 computational time.

194 Data sets are often designated with too many variables for effective model structure (Miron
195 & Witold, 2010). Commonly most of these variables are extraneous to the classification, and
196 perceptibly their relevance is unknown in advance (Miron & Witold, 2010). Several difficulties
197 arise while dealing with large feature sets. One is decently technical — dealing with large feature
198 sets impedes computational speed, consumes too many resources and is merely bothersome.

199 Another is even more important — many machine learning algorithms reveal a diminution of
200 accuracy when the number of variables is considerably higher than optimal (Ron & George, 1997).
201 Therefore, selection of minimal feature set that can yield the best possible classification outcome
202 is needed for practical reasons (Miron & Witold, 2010). This problem also known as the minimal-
203 optimal problem (Nilsson, Peña, Björkegren, & Tegner, 2007), has been intensively analyzed and
204 there are several algorithms which are established to reduce the feature set to a manageable and
205 optimal size (Miron & Witold, 2010).

206 Nevertheless, this genuine goal sleuths another problem — the identification of all
207 attributes which are in certain circumstances germane for classification, the so-called "all-relevant
208 problem" (Miron & Witold, 2010). Finding all relevant attributes, instead of the non-redundant
209 ones, may be beneficial. This is essential when one is involved in understanding the fundamental
210 mechanisms related to the subject of interest, instead of purely building a black box prognostic
211 model. For example, when dealing with classification of Mesothelioma dataset, identification of
212 all predictors which are related to the outcome ("Healthy" or "Diseased") is necessary for complete
213 understanding of the process, whereas a minimal-optimal set of predictors (variables) might be
214 more useful as classification markers. An honest discussion demarcating the importance of finding
215 relevant attributes is given by Nilsson et al. in 2007 (Nilsson, Peña, Björkegren, & Tegner, 2007).

216 The phase-2 of our study implements Boruta algorithm for selecting all relevant predictor
217 (Choudhury & Greene, Evaluating Patient Readmission Risk: A Predictive Analytics Approach,
218 2018). Boruta algorithm is a wrapper built around the random forest classification algorithm
219 (Miron & Witold, 2010) implemented in the R random forest package (Liaw & Wiener, 2002).
220 Boruta algorithm uses Z-score as the importance measure since it considers the fluctuations of the

221 mean accuracy loss among trees in the forest (Miron & Witold, 2010). Since we cannot use Z-
222 score unswervingly to gauge importance, an external reference is needed to decide whether the
223 importance of any given attribute is significant. To determine the importance of each attribute
224 Boruta algorithm creates an analogous ‘shadow’ attribute, whose values are obtained by shuffling
225 values of the original attribute across objects (Miron & Witold, 2010). Then a classification is
226 performed using all the attributes of the extended system to calculate the importance of all
227 variables. The importance of a shadow attribute can be nonzero purely due to random fluctuations
228 (Miron & Witold, 2010). Thus, the set of the importance of shadow attributes is used as a reference
229 for determining essential attributes (Miron & Witold, 2010).

230 The following algorithms were implemented, compared and tested using *paired T –*
231 *test (corrected)* at 0.05 significance.

232 **3.1. Algorithms**

233 **Stochastic Gradient Descent (SGD)**

234 Gradient descent is a method to determine the local minima. Stochastic gradient descent is
235 gradient descent performed using multiple updates at a time on a small batch (minibatch) of the
236 dataset selected at random (stochastically). Instead of calculating the gradient of the cost (error)
237 based on the whole dataset, SGD break the dataset into mini batches and compute the gradient on
238 each batch separately followed by a neural net update based on the partial gradient. In other words,
239 it is an optimization algorithm that iteratively determines the values of learnable parameters of a
240 function (f) to minimize the cost function (error rate). Cost function for our study is root mean
241 squared error, which can be determined using the following equation (eq.1).

242
$$RMSE = \sqrt{\frac{1}{N} \sum_{i=1}^n (y_i - (mx_i + b))^2} \quad (1)$$

243 Mathematically, SGD is a simplification of gradient descent. Instead of calculating the
 244 gradient of $E_n(f_w)$ (empirical risk using gradient descent), each iteration estimates this gradient
 245 by a single randomly picked example (eq.2):

246
$$z_t: w_{t+1} = w_t - \gamma_t \nabla_w Q(z_t, w_t). \quad (2)$$

247 Where z is a random pair of input x and scalar output y ; w is weight; γ is learning rate;
 248 $Q(z, w)$ is the loss. Since the stochastic algorithm does not require to retain which examples were
 249 visited during the previous iterations, it can process examples on the fly in a deployed system.

250 **Adaptive Boosting M1**

251 It is also known as AdaBoost.M1, is a machine learning meta-algorithm that can be
 252 implemented in conjunction with other types of learning algorithms to convalesce performance.
 253 The output of the other learning algorithms ('weak learners') is merged into a weighted sum that
 254 epitomizes the final output of the boosted classifier. AdaBoost is adaptive since it can fine-tune
 255 the weak learners in favor of misclassified instances by previous classifiers. AdaBoost-M1 refers
 256 to a specific method of training a boosted classifier (eq.3).

257
$$F_T(x) = \sum_{t=1}^T f_t(x) \quad (3)$$

258 Where T is the number of iterations; each f_t is a weak learner that takes an object x as input
 259 and returns a value indicating the class of the object. Each weak learner produces an output

260 hypothesis, $h(x_i)$, for each sample in the training set. At each iteration t , a weak learner is selected
261 and assigned a coefficient α_t such that the sum of training error E_t (eq.4) of the resulting t -stage
262 boost classifier is minimized.

$$263 \quad E_t = \sum E|F_{t-1}(x_i) + \alpha_t h(x_i) \quad (4)$$

264 Where $F_{t-1}(x)$ is the boosted classifier that has been built up to the previous stage of
265 training. $E(F)$ is some error function, and $f_t(x) = \alpha_t h(x)$ is the weak learner that is being
266 considered for addition to the final classifier.

267 **Kernel Logistic Regression (KLR)**

268 It is a well-established statistical model for classification. Unlike Logistic Regression, KLR
269 enables the classification of linearly non-separable problems by assigning the input variables to a
270 higher dimensional space, via the kernel trick. The kernel is a conversion function that must satisfy
271 mercer's necessary and sufficient conditions, which state that a kernel function must be expressed
272 as an inner product and must be positive semidefinite.

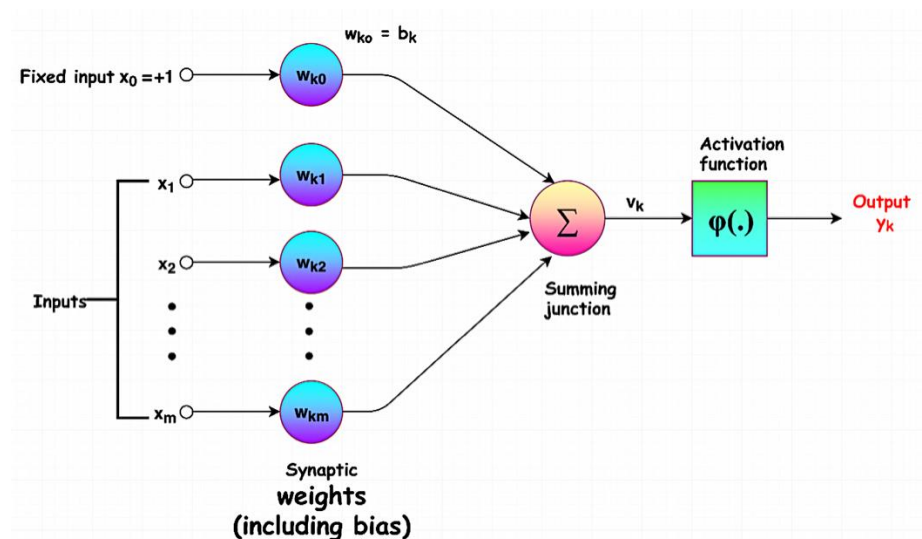
273 **Multi-layer Perceptron**

274 The Artificial Neural Network (ANN), also known as a neural network, is a computational
275 prototype based on the biological neural network. Its fundamental theory originated in the
276 connectionism of cognitive science in which several simple computational units are linked to show
277 intelligent compartments. Such a concept is germane to the neurons of the biological neural system
278 and the computational units of computational prototypes. A typical ANN comprises of an input
279 layer, hidden layer(s), and an output layer. The first layer known as the input layer consists of a

280 neuron set $\{x_i|x_1, x_2, \dots, x_m\}$ denoting the input variables. Each neuron in the hidden layer
 281 transforms the values from the preceding layer with a weighted linear summation $w_1x_1 + w_2x_2 +$
 282 $\dots + w_mx_m$, Followed by a non-linear activation function such as hyperbolic tan function. The
 283 output layer receives the values from the last hidden layer and transforms them into the output
 284 values.

285 Figure 1 shows a typical neuron model, which is comprised of two parts. The first part is
 286 the accretion of signals, where the input signals (input data) are gathered for a sum. As shown in
 287 the following equation (eq.5), each weight (w_i) equals a data dimension (x_i), while (w_0) as a bias is
 288 correspondent to the intercept or constant term of the function. While the constant is set to "1" as
 289 the input of 0th dimension, the bias is managed as the weight of 0th dimension. This is also called
 290 affine transformation (Lee, Chen, Yu, & Lai, 2018).

291
$$Z = bias + \sum_{i=1}^m X_i W_i = \sum_{i=0}^m X_i W_i \quad (5)$$

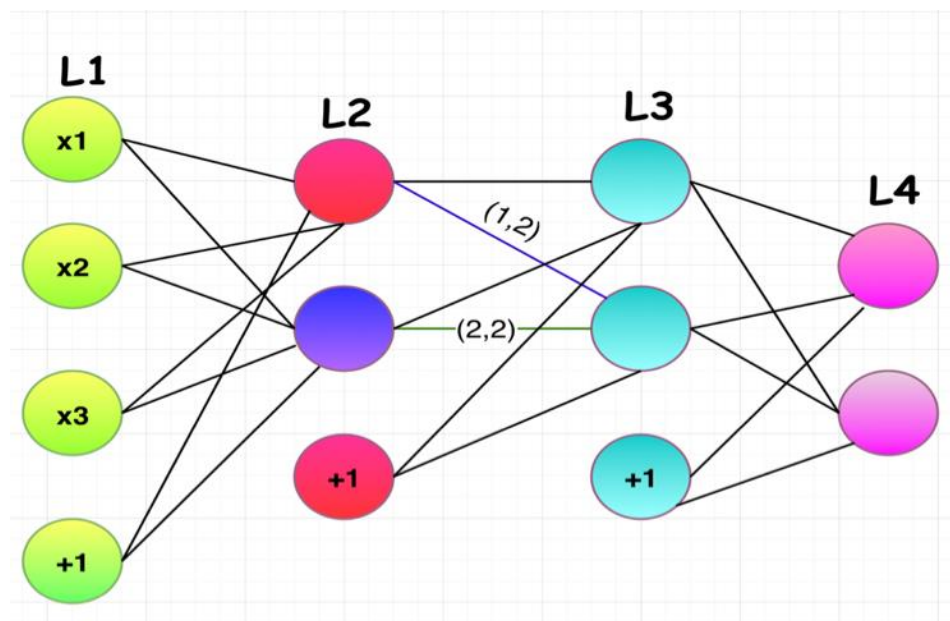


292

293

Figure 1. Typical neural network

294 The second part is the initiation of the function, where the obtained activation value is used
295 for the nonlinear compressed transformation to extricate a nonlinear eigenvalue. The frequently-
296 used activation functions include ReLU, Sigmoid, and Tanh (Lee, Chen, Yu, & Lai, 2018). A
297 neural network is a network based on the interconnection between artificial neurons. The
298 feedforward neural network (FNN) or multilayer perceptron (MLP) is a neural network that
299 permits the feedforward connection of neurons. The input of data is known as the input layer, while
300 the output of results is termed as the output layer; the layers between the input layer and the output
301 layer are called the hidden layers (Lee, Chen, Yu, & Lai, 2018). MLP is a supervised algorithm
302 that learns a function $f(\cdot): R^m \rightarrow R^o$ by training on a given dataset, where m is the dimension for
303 input and O is the output dimension. Provided a set of features $X = x_1, x_2, x_3, \dots, x_m$ and target y ,
304 it can learn a non-linear function for either classification or regression.



305

306

Figure 2. Feed-forward neural network

307 Figure 2 shows a 4 layered neural network, where the first layer (L1) is the input layer; L2
 308 and L3 are the hidden layers; L4 is the output layer; $a_{i,j}^{(l)}$ refers to the connection weight of “ i ”
 309 (ordinal number) neuron on layer I and “ j ” (ordinal number) neural on layer $I+1$; a_j^I denotes the
 310 connection between the bias on layer I and “ j ” neuron on layer $I+1$; and a_j^I implies the activation
 311 value (output value) of the “ I ” neuron on layer I , and the activation value of the blue neuron in the
 312 picture is $a_2^{(2)}$ (Lee, Chen, Yu, & Lai, 2018).

313 Voted Perceptron (VP)

314 It is designed for linear classification, that combines the Rosenblatt's perception algorithm
 315 with Helmbold and Warmuth's leave-out method. All weight vectors confronted during the
 316 learning process vote on a prediction. The measure of the accuracy of a weight vector, based on
 317 the number of trials in which it correctly classifies instances, is used as the number of votes given
 318 to the weight vector. The output a voted perceptron is given by (eq.6) when given labeled data is
 319 (x_i, y_i) where y is $+1$ or -1 (mesothelioma or healthy):

$$320 \quad y_i = \text{sign} \left\{ \sum_{p=0}^P c_p \text{sign}(w_p, x) \right\} \quad (6)$$

321 Where x are inputs, $p = 0, 1, 2, \dots, P$; w_p are weights, y_i is the predicted class, and c_p is
 322 the survival time (reliability of w_p).

323 Hoeffding Tree

324 It is also known as Very Fast Decision Tree (VFDT) is a tree algorithm for data stream
 325 classification. The Hoeffding tree is an incremental decision tree learner for a large dataset, that
 326 assumes that the data distribution is constant over time. It grows a decision tree based on the
 327 theoretical guarantees of the Hoeffding bound. In other words, VFDT employs Hoeffding bound
 328 to decide the minimum number of arriving instances to achieve a certain level of confidence in
 329 splitting the node. The confidence level determines the proximity of the statistics between the
 330 attribute chosen by VFDT and the attribute chosen by decision tree for batch learning.

331 Clojure Classifier (CC)

332 It is a wrapper classifier developed in Clojure programming language. It mandates to have
 333 at least a learn-classifier function and distribution-for-instance function. The learn-classifier
 334 function takes an object and a string (nullable) and returns the learned model as a serializable data
 335 structure. The distribution-for-instance function takes an instance to be predicted and a model as
 336 an argument and returns the prediction as an array.

337 2.1.1. Primal Estimated sub-Gradient Solver for SVM

338 It is also known as s-Pegasos. It performs SGD on a primal objective (eq. 7,8) with
 339 carefully chosen step size.

$$340 \min_w \frac{\lambda}{2} \|W\|^2 + \frac{1}{m} \sum_{(x,y) \in S} l(W; (X, y)) \quad (7)$$

341 Where

$$342 l(w; (X, y)) = \max\{0, 1 - y(w, X)\} \quad (8)$$

343 3.2.Model evaluation

344 While evaluating supervised machine learning models, it is important to measure each model's
345 classification *accuracy, f-measure, recall, precision, root mean squared error (RMSE), receiver*
346 *operating characteristic (ROC), and precision-recall curve (PRC).*

347 Classification accuracy is the metric for evaluating classification models. It is the fraction of
348 predictions or classification that a model performs correctly. Classification accuracy can be
349 calculated by the given equation (eq.9)

$$350 \quad Accuracy = \frac{\text{Number of correct prediction}}{\text{Total number of prediction}} = \frac{TP + TN}{TP + TN + FP + FN} \quad (9)$$

351 Where TP = True positive; TN = True negative; FP = False positive; FN = False negative.

352 The ROC curve is the graphical representation of the true positive rate (TPR) against the
353 false positive rate (FPR) at different threshold settings. In the machine learning domain, a TPR is
354 also known as sensitivity, recall or "probability of detection." Similarly, an FPR is known as the
355 fall-out or "probability of false alarm" and can be calculated as (eq. 10). The ROC curve is thus
356 the sensitivity as a function of fall-out.

$$357 \quad FPR = (1 - specificity) \quad (10)$$

358 Regarding information retrieval undertakings with binary classification (relevant or not
359 relevant), precision is the segment of retrieved instances that are relevant, whereas recall, also
360 known as sensitivity is the fraction of retrieved instances to all relevant instances. In this context
361 of information retrieval, the PRC becomes very useful. PRC is a graphical representation of recall

362 (x-axis) and precision (y-axis), where recall and precision are determined using the given formula
363 (eq. 11,12) respectively.

$$364 \quad \text{Recall} = \frac{TP}{(TP + FN)} \quad (11)$$

$$365 \quad \text{Precision} = \frac{TP}{(TP + FP)} \quad (12)$$

366 *f-measure*, also known as F1-score is the harmonic mean of precision and recall (eq.13), where *f-*
367 *measure* reaches its best at 1 and worst at 0.

$$368 \quad f1 \text{ score} = \frac{2 * (\text{precision} * \text{recall})}{\text{precision} + \text{recall}} \quad (13)$$

369 The root-mean-square error (RMSE) is a measure of performance of a model. It does this
370 by computing the difference between predicted and the actual values as given below (eq. 14).

$$371 \quad RMSE = \sqrt{\sum_{i=1}^N \frac{(x_i - y_i)^2}{N}} \quad (14)$$

372 Where $(x_i - y_i)$ is the difference between predicted and actual value and N is the sample size.

373 4. Results

374 Phase 1

375 As shown in table 2, SGD, AdaBoost.M1, KLR, MLP, VFDT generates perfect results with
376 100% accuracy, precision, recall, and f-measure. These algorithms also return the highest possible
377 ROC, PRC, and zero RMSE. s-Pegasos also delivers close to the optimal result.

378 In this phase, the high accuracy of 100% indicates that results obtained from biopsy and
 379 imaging tests are very strong predictors of MM. This result validates the significance of biopsy
 380 and imaging results ("diagnosis method") from a data science viewpoint.

381 Table 2. Comparing classification accuracy (phase-1)

| Algorithm | SGD | AdaBoost.M1 | KLR | MLP | VP | VFDT | CC | s-Pegasos |
|------------------------------------|------|-------------|------|------|-------|------|-------|-----------|
| Classification accuracy (%) | 100 | 100 | 100 | 100 | 70.38 | 100 | 70.38 | 99.36 |
| f-measure | 1.00 | 1.00 | 1.00 | 1.00 | 0.83 | 1.00 | 0.83 | 1.00 |
| Recall | 1.00 | 1.00 | 1.00 | 1.00 | 1.00 | 1.00 | 1.00 | 1.00 |
| Precision | 1.00 | 1.00 | 1.00 | 1.00 | 0.70 | 1.00 | 0.70 | 0.99 |
| ROC | 1.00 | 1.00 | 1.00 | 1.00 | 0.50 | 1.00 | 0.50 | 0.99 |
| PRC | 1.00 | 1.00 | 1.00 | 1.00 | 0.70 | 1.00 | 0.70 | 0.99 |
| RMSE | 0.00 | 0.00 | 0.00 | 0.00 | 0.54 | 0.01 | 0.54 | 0.04 |

382

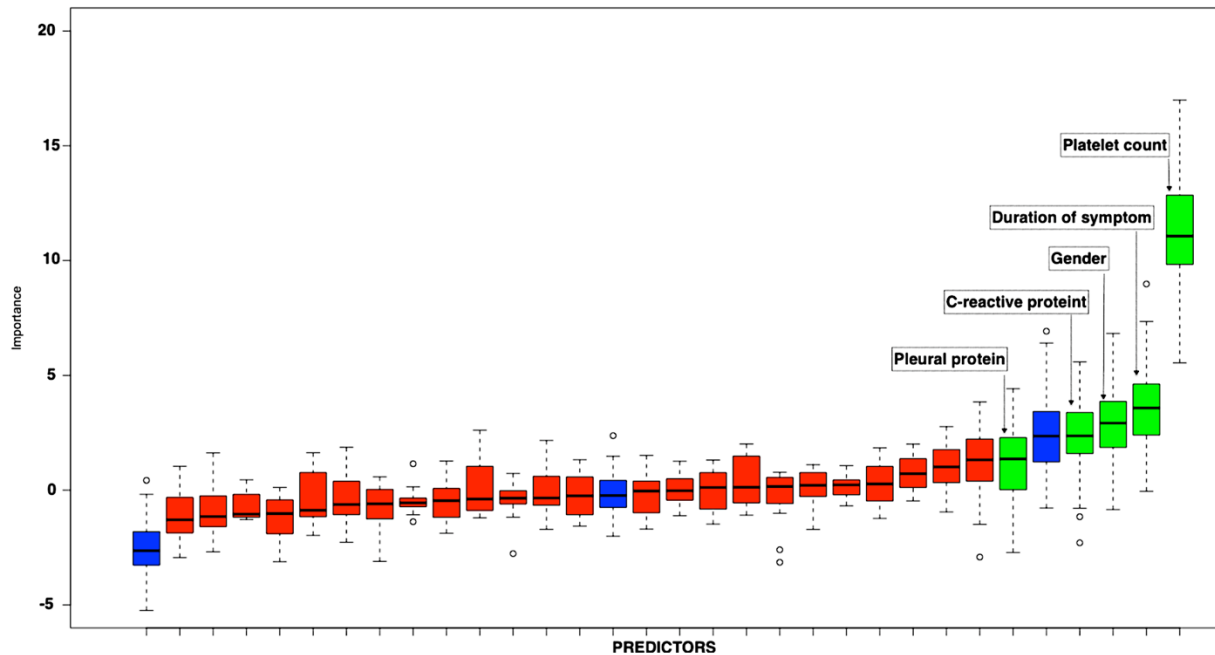
383 Phase 2 demonstrates the relevance of pre-diagnosis data. It also shows the behavior of all
 384 predicting models post removal of "diagnosis method" and other post-diagnosis data.

385 Phase 2

386 Boruta algorithm confirmed five relevant attributes that are enough to predict the presence
 387 of Mesothelioma without any loss in model's performance. In other words, the selected attributes
 388 alone can prognosticate MM with the same accuracy as all other pre-diagnosis predictors when
 389 taken together as input. The relevant predictor identified were *c-reactive protein*, *platelet count*,
 390 *duration of symptoms*, *gender*, and *pleural protein*.

391 This method neither downgrades the remaining predictors nor does it recommend revising
 392 the regular clinical procedures. Figure 3 below shows the attributes recognized by Boruta
 393 algorithm. Boruta plot generates a box plot for each attribute. The x-axis represents each of

394 candidate explanatory variables. The green box plots refer to the relevant attributes whereas the
 395 red ones are identified as unimportant (from a data science viewpoint). The blue boxplots
 396 correspond to minimal, average and maximum Z score of a shadow attribute created by the Boruta
 397 algorithm. The following table 3 compares the different performance measures of each algorithm
 398 used in this study.



399

400

Figure 3. Boruta plot for feature selection

401 AdaBoost outperformed all other models with the highest classification accuracy of
 402 71.29%. Excluding “diagnosis method” from the prediction model resulted in decreased accuracy.
 403 However, this phase has its own advantage. Despite lower accuracy, phase-2 helps reducing
 404 diagnostic expenses.

405

Table 3. Comparing classification accuracy (phase-2)

| Algorithm | SGD | AdaBoost.M1 | KLR | MLP-C | VP | VFDT | CC | s-Pegasos |
|------------------------------------|-------|-------------|-------|-------|-------|-------|-------|-----------|
| Classification accuracy (%) | 69.23 | 71.29 | 69.51 | 64.11 | 70.38 | 70.38 | 70.38 | 67.03 |
| f-measure | 0.80 | 0.82 | 0.79 | 0.74 | 0.83 | 0.83 | 0.83 | 0.77 |

| | | | | | | | | |
|------------------|------|------|------|------|------|------|------|------|
| Recall | 0.80 | 0.86 | 0.93 | 0.84 | 1.00 | 1.00 | 1.00 | 0.81 |
| Precision | 0.74 | 0.74 | 0.76 | 0.75 | 0.70 | 0.70 | 0.70 | 0.75 |
| ROC | 0.58 | 0.61 | 0.65 | 0.61 | 0.50 | 0.50 | 0.50 | 0.58 |
| PRC | 0.74 | 0.77 | 0.82 | 0.79 | 0.70 | 0.70 | 0.70 | 0.74 |
| RMSE | 0.55 | 0.45 | 0.46 | 0.57 | 0.54 | 0.46 | 0.54 | 0.57 |

406

407 **Discussion**

408 An accurate diagnosis of MM is crucial at both the individual and public health level. It
 409 has necessary medicolegal significance due to diagnosis-related compensation (Ascoli, 2015).
 410 However, prognosticating MM is challenging due to its composite epithelial pattern and low
 411 likelihood of occurrence (Ascoli, 2015). To advocate the prognosis of MM with high accuracy and
 412 low diagnostic cost, the current study designed and implemented a prediction model comprising
 413 of two phases. (phase 1 and 2).

414 To our knowledge no previous studies have implemented our AI models and focused on
 415 reducing diagnosis expenses by eliminating biopsy and imaging test results from the dataset.
 416 Phase-2 of our study proposes AdaBoost.M1 algorithm that can identify high risk patients at lower-
 417 cost by taking only blood test results and patient's demographic data. Outcome from phase-2 can
 418 provide the doctors with a list of high-risk patients. Doctors and other healthcare providers can
 419 then prescribe biopsy tests only to the identified patients for reconfirming MM using phase-1
 420 model with optimal accuracy. This approach will reduce unnecessary biopsy tests and thus reduce
 421 overall expenses by up to \$7900 (Molinari, 2018).

422 The recommended model (AdaBoost) in phase-2 requires *c-reactive protein*, *platelet count*,
 423 *duration of symptoms*, *gender*, and *pleural protein* as its input. The expenses to collect the required
 424 input data can range from. \$100 to \$200 (Practo, 2017) for Protein Total Pleural Fluid (*pleural*

425 *protein*), \$40 to \$70 (Haiken, 2011) for c-reactive protein test, and \$6 to \$167 (Pinder, 2012) for
426 complete blood count (*platelet* count) depending up on the location. These factors can also
427 advocate early prognosis of MM; Moreover, studies have shown that higher (>1 mg/dL) c-reactive
428 protein influences mesothelioma (Takamori, et al., 2018) (Ghanim, et al., 2012), another study at
429 the University of Maryland determined the clinical significance of preoperative thrombocytosis
430 (high count of platelets), in patients with MPM (Li, et al., 2017).

431 **5. Conclusion**

432 Our study identifies that the *diagnosis method* (biopsy and imaging test results), *c-reactive protein*,
433 *platelet count*, *duration of symptoms*, *gender*, and *pleural protein* plays a significant role in
434 diagnosing MM. However, effective diagnosis methods such as pleuroscopy (lungs) or
435 laparoscopy (abdomen), thoracotomy (lungs) or laparotomy (abdomen), and imaging tests (CT
436 scan and MRI) are expensive. This study proposes two approaches to predict MM, each having its
437 advantages and limitations. The first approach (phase-1) uses all predictors from mesothelioma
438 data and produces 100% classification accuracy. The second approach (phase-2) ensures cost
439 reduction. Our study recommends AdaBoost algorithms for MM prognosis and suggests using
440 phase-2 approach to short list high risk patients followed by phase 1 to confirm MM.

441

442

443

444

445

446

447

448

449

450

451

452

453

454 **List of abbreviations**

455 • MPM – Malignant Pleural Mesothelioma

456 • MM – Malignant Mesothelioma

457 • PM – Pleural Mesothelioma

458 • ROC – Receiver Operating Characteristics

459 • PRC – Precision-recall curve

460 • DT – Decision tree

461 • VFDT – Very fast decision tree

462 • MLP – Multi-layer perceptron

463 • SGD – Stochastic gradient descent

464 • KLR – Kernel logistic regression

465 • AdaBoost – Adaptive boosting

466 • RMSE – Root mean squared error

467 • ANN – Artificial neural network

468 • SVM – Support vector machine

469 • S-Pegasos - Primal Estimated sub-Gradient Solver for SVM

470 • CC – Clojure classification

- 471 • VP – Voted perceptron
- 472 • TP – True positive
- 473 • TN – True negative
- 474 • FP – False positive
- 475 • FN – False negative
- 476 • TPR – True positive rate
- 477 • FPR – False positive rate
- 478 • WBC – White blood cell
- 479 • HGB – Hemoglobin
- 480 • PLT – Platelet count
- 481 • LDH – Blood lactic dehydrogenase
- 482 • ALP – Alkaline phosphate
- 483 • CRP – C reactive protein
- 484 • AUC – Area under the curve

485 **Declarations**

- 486 - Ethics approval and consent to participate - All data were collected with the permission of the
487 organization and the study ensure no leakage of any patient's medical and personal
488 information.
- 489 - Consent for publication - Not applicable
- 490 - Availability of data and material - All data analyzed during this study are included in this
491 published article and its supplementary information files.
- 492 - Competing interests - The authors declare that they have no competing interests
- 493 - Funding - Any internal or external source did not fund this study

494 - Authors' contribution - AC analyzed, interpreted the mesothelioma data. AC performed the
495 time series forecasting and evaluated the model.

496 - Acknowledgments - Not applicable

497 -

498 **Reference**

499 Ascoli, V. (2015). Pathologic diagnosis of malignant mesothelioma: Chronological prospect and
500 advent of recommendations and guidelines. *Ann Ist Super Sanità*, 51(1), 52-59.

501 Bueno, R., Stawiski, E., Goldstein, L., & al., e. (2016;). Comprehensive genomic analysis of
502 malignant pleural mesothelioma identifies recurrent mutations, gene fusions and splicing
503 alterations. *Nat Genet*, 48, 407–416.

504 Choudhury , A. (2018). Identification of Cancer: Mesothelioma's Disease Using Logistic
505 Regression and Association Rule. *American Journal of Engineering and Applied Sciences*,
506 11(4), 1310-1319.

507 Choudhury, A., & Greene, C. (2018). Evaluating Patient Readmission Risk: A Predictive Analytics
508 Approach. *American Journal of Engineering and Applied Sciences*, 11(4), 1320-1331.

509 Frauenfelder, T., Tutic, M., Weder, W., & al., e. (2011;). Volumetry: an alternative to assess
510 therapy response for malignant pleural mesothelioma? *Eur Respir J .*, 38, 162-168.

511 Friedin, R. B. (2012, May 11). *Am I going to die because I cannot afford the test?* (KevinMD)
512 Retrieved December 26, 2018, from [https://www.kevinmd.com/blog/2012/05/die-afford-](https://www.kevinmd.com/blog/2012/05/die-afford-test.html)
513 [test.html](https://www.kevinmd.com/blog/2012/05/die-afford-test.html)

514 Ghanim, B., Hoda, M. A., Winter, M.-P., Klikovits, T., Alimohammadi, A., Hegedus, B., . . .
515 Berger, W. (2012). Pretreatment serum C-reactive protein levels predict benefit from

- 516 multimodality treatment including radical surgery in malignant pleural mesothelioma: a
517 retrospective multicenter analysis. . *Annals of Surgery*, 256(2), 357–362.
- 518 Gill, R., Naidich, D., Mitchell, A., & al., e. (2016;). North American multicenter volumetric CT
519 study for clinical staging of malignant pleural 30. mesothelioma: feasibility and logistics
520 of setting up a quantitative imaging study. . *J Thorac Oncol* , 11, 1335–1344.
- 521 Haiken, M. (2011, July 17). *3 New Medical Tests that Can Save Your Life - But You Have to Ask*.
522 (Forbes) Retrieved December 26, 2018, from
523 [https://www.forbes.com/sites/melaniehaiken/2011/06/17/3-lifesaving-new-medical-tests-](https://www.forbes.com/sites/melaniehaiken/2011/06/17/3-lifesaving-new-medical-tests-you-have-to-ask-for/#2df47f75398a)
524 [you-have-to-ask-for/#2df47f75398a](https://www.forbes.com/sites/melaniehaiken/2011/06/17/3-lifesaving-new-medical-tests-you-have-to-ask-for/#2df47f75398a)
- 525 Ilhan, H. O., & Celik, E. (2016). The mesothelioma disease diagnosis with artificial intelligence
526 methods. *2016 IEEE 10th International Conference on Application of Information and*
527 *Communication Technologies*. Baku.
- 528 James, G., Witten, D., Hastie, T., & Tibshirani, R. (2017). *An Introduction to Statistical Learning:*
529 *with Applications in R*. New York: Springer.
- 530 Kuhn, M., & Johnson, K. (2018). *Applied Predictive Modeling*. New York: Springer.
- 531 Lee, S.-J., Chen, T., Yu, L., & Lai, C.-H. (2018). Image Classification Based on the Boost
532 Convolutional Neural Network. *IEEE Access*, 6, 12755-12768.
- 533 Leigh, J., Corvalan, C., Grimwood, A., Berry, G., Ferguson, D., & al., e. (1991;). The incidence
534 of malignant mesothelioma in Australia 1982–1988. *Am J Ind Med* , 20, 643–655.
- 535 Li, Y. C., Khashab, T., Terhune, J., Eckert, R. L., Hanna, N., Burke, A., & Alexander, H. R. (2017).
536 Preoperative Thrombocytosis Predicts Shortened Survival in Patients with Malignant
537 Peritoneal Mesothelioma Undergoing Operative Cytoreduction and Hyperthermic
538 Intraperitoneal Chemotherapy. *Annals of Surgical Oncology*, 24(8), 2259–2265.

- 539 Liaw, A., & Wiener, M. (2002). Classification and Regression by random Forest. *R News*, 2(3),
540 18-22.
- 541 Lotfi, E., & Keshavarz, A. (2014). Gene expression microarray classification using PCA-BEL.
542 *Computers in Biology and Medicine*, 54, 180-187.
- 543 McDonald, C., J., & McDonald., A. D. (1996). The epidemiology of mesothelioma in historical
544 context. . *European Respiratory Journal* , 9, 1932-1942.
- 545 Mesothelioma News. (2018, July 28). *What Mesothelioma Does to the Body*. Retrieved August 25,
546 2018, from [http://www.mesotheliomanews.com/medical/mesothelioma-diagnosis/pleural-](http://www.mesotheliomanews.com/medical/mesothelioma-diagnosis/pleural-mesothelioma/)
547 [mesothelioma/](http://www.mesotheliomanews.com/medical/mesothelioma-diagnosis/pleural-mesothelioma/)
- 548 Metintas, M., Metintas, S., Guntulu AK, S. E., Alatas, F., Kurt, E., Uugun, I., & Yildirim, H.
549 (2008). Epidemiology of pleural mesothelioma in a population with non-occupational
550 asbestos exposure. *Respirology*, 13, 117-121.
- 551 Miron, B. K., & Witold, R. R. (2010). Feature Selection with the Boruta Package. *Journal of*
552 *Statistical Software*, 36(11), 2-13.
- 553 Molinari, L. (2018, November Thursday). *Mesothelioma Treatment Costs*. (Cancer Alliance)
554 Retrieved December Saturday, 2018, from
555 <https://www.mesothelioma.com/treatment/mesothelioma-treatment-costs/>
- 556 Nilsson, R., Peña, J. M., Björkegren, J., & Tegner, J. (2007). Consistent Feature Selection for
557 Pattern Recognition in Polynomial Time. *The Journal of Machine Learning Research*, 8,
558 612.
- 559 Pass, H., Giroux, D., Kennedy, C., & al., e. (2016). The IASLC mesothelioma staging project:
560 improving staging of a rare disease through 29. international participation. *J Thorac Oncol*,
561 11, 2082-2088.

- 562 Paydar, K., R. S., Kalhori, N., Akbarian, M., & Sheikhtaheri, A. (2017). A clinical decision
563 support system for prediction of pregnancy outcome in pregnant women with systemic
564 lupus erythematosus. *International Journal of Medical Informatics* , 97, 239-246.
- 565 Peto, J., Hodgson, J., Matthews, K., & Jones, J. (1995;). Continuing increase in mesothelioma
566 mortality in Britain. *Lancet*, 345, 535–539.
- 567 Pinder, J. (2012, December 27). *How much does a blood test cost? It could be \$6, or \$167* . (Clear
568 Health Cost Beta) Retrieved December 26, 2018, from
569 [https://clearhealthcosts.com/blog/2012/12/how-much-does-a-blood-test-cost-it-could-be-](https://clearhealthcosts.com/blog/2012/12/how-much-does-a-blood-test-cost-it-could-be-16-or-117/)
570 [16-or-117/](https://clearhealthcosts.com/blog/2012/12/how-much-does-a-blood-test-cost-it-could-be-16-or-117/)
- 571 Pope, T. P. (2010, February 4). *When Patients Can't Afford Their Care*. (New York Times)
572 Retrieved December 26, 2018, from [https://well.blogs.nytimes.com/2010/02/04/when-](https://well.blogs.nytimes.com/2010/02/04/when-patients-cant-afford-their-care/)
573 [patients-cant-afford-their-care/](https://well.blogs.nytimes.com/2010/02/04/when-patients-cant-afford-their-care/)
- 574 Practo. (2017, December 11). *Protein Total Pleural Fluid*. Retrieved December 25, 2018, from
575 <https://www.practo.com/tests/protein-total-pleural-fluid/p>
- 576 Ron, K., & George, H. J. (1997). Wrappers for feature subset selection. *Artificial Intelligence*, 97,
577 273-324.
- 578 Selby, K. (2018, December 20). *Mesothelioma Diagnosis* . (Asbestos.com and The Mesothelioma
579 Center) Retrieved December 22, 2018, from
580 <https://www.asbestos.com/mesothelioma/diagnosis/>
- 581 Silvester, J. (2016, September 27). *Most of the World Doesn't Have Access to X-Rays*. (Health)
582 Retrieved December 26, 2018, from
583 <https://www.theatlantic.com/health/archive/2016/09/radiology-gap/501803/>

- 584 Spirtas, R., Beebe, G., Connelly, R., Wright, W., Peters, J., & al., e. (1986;). Recent trends in
585 mesothelioma incidence in the United States. *Am J Ind Med*, 9, 397-407.
- 586 Stefano, P., Rosa, F., & Paola, M. e. (2015). Differential diagnosis of pleural mesothelioma using
587 Logic Learning Machine. *BMC Bioinformatics* , 16, 1471-2105.
- 588 Takamori, S., Toyokawa, G., Shimokawa, M., Kinoshita, F., Kozuma, Y., Matsubara, T., . . . et.al.
589 (2018). The C-Reactive Protein/Albumin Ratio is a Novel Significant Prognostic Factor in
590 Patients with Malignant Pleural Mesothelioma: A Retrospective Multi-institutional Study
591 . *Ann Surg Oncol*, 25(17), 1-8.
- 592 Tin, K. (1995). Random decision forests. *Proceedings of 3rd International Conference on*
593 *Document Analysis and Recognition*. Montreal.
- 594 Vogelzang, N., Rusthoven, J., Symanowski, J., & al., e. (2003). Phase III study of pemetrexed in
595 combination with cisplatin versus cisplatin alone in patients with malignant pleural
596 mesothelioma. *J Clin Oncol* 2003; 21:2636–44., 21, 2636-2644.
- 597 Zalcman, G., Mazieres, J., Margery, J., Greillier, L., Audigier-Valette, C., Moro-Sibilot, D., . . .
598 et.al. (2016). Bevacizumab for newly diagnosed pleural mesothelioma in the Mesothelioma
599 Avastin Cisplatin Pemetrexed Study (MAPS): a randomised, controlled, open-label, phase
600 3 trial. *Lancet*, 387, 1405-1414.

601

602

603 **List of figure legends**

604 **Figure 4:** Typical neural network

605 **Figure 2:** Feed-forward neural network

606 **Figure 3:** Boruta plot for feature selection.